Fusion Engineering and Design 171 (2021), 112598, DOI: 10.1016/j.fusengdes.2021.112598

Conceptual design overview of the ITER WCLL Water Cooling System and supporting thermal-hydraulic analysis

C. Ciurluini[a], V. Narcisi[a], A. Tincani[b], C. Ortiz Ferrer[c], F. Giannetti[a]

[a] *Sapienza University of Rome, Department of Astronautical, Electrical and Energy Engineering (DIAEE), Italy*

[b] *ENEA FSN-ING CR Brasimone, 40032 Camugnano (BO), Italy*

[c] *F4E at ITER Organization, Route de Vinon-sur Verdon, 13115 St Paul lez Durance, France*

Abstract

In this paper, the conceptual design of the International Thermonuclear Experimental Reactor (ITER) Water-Cooled Lithium-Lead (WCLL) Test Blanket Module (TBM) Water Cooling System (WCS) from Europe is presented. The system consists of two loops in series. This design feature allows the removal of heat from the TBM box avoiding at the same time the release of radionuclides into the ITER Component Cooling Water System (CCWS), that acts as WCLL Test Blanket System heat sink. For this purpose, the WCS primary loop deals with the direct heat removal from the ITER TBM and the secondary one implements physical separation between the contaminated primary loop coolant and the CCWS. The insertion of an economizer into the primary loop determines the characteristic “eight” shape of the circuit. This choice was done in order to reduce the temperature difference on the intermediate heat exchanger. Hairpin type and steam bubble are the technologies selected for heat exchangers and pressurizers, respectively. Pressure and temperature control systems are foreseen to limit excursions from rated values in normal operational states and abnormal transients.

A computational activity was promoted to assess the WCLL-WCS conceptual design, using a modified version of the RELAP5 Mod3.3 system code. A detailed thermal-hydraulic model was developed on the basis of design outcomes. The nodalization scheme includes the TBM, the WCS, a portion of the CCWS and the lithium-lead circuit. The computational campaign involved both the normal operational state and selected abnormal transients. In all the scenarios simulated, the conceptual design has highlighted the capability of operating the system respecting all the thermal-hydraulic requirements. The abnormal transient selected and presented is the loss of flow in the CCWS (loss of heat sink). In these conditions, TBM cooling function has been verified, keeping standard control strategies without any external action.

Keywords: ITER, TBM, WCS, RELAP5, LOHS

1 Framework and state of the art

The Water-Cooled Lithium Lead (WCLL) Breeding Blanket (BB) is one of the two main R&D strategies investigated for the European (EU) Demonstration Fusion Power Plant (DEMO) [1]. The other option considered is the Helium-Cooled Pebble Bed (HCPB) [2]. These two technologies will be preliminary tested in the International Thermonuclear Experiment Reactor (ITER), according to the goals of the ITER Test Blanket Module (TBM) programme [3] [4]. The main outcome of this experimental campaign will be the return of experience for the EU-DEMO Breeding Blanket Programme [5]. Through the design, manufacturing, and operation of WCLL and HCPB Test Blanket Systems (TBS), the TBM programme aims at demonstrating the feasibility of the most promising BB candidates for DEMO reactor, as well as their compliance to some selected high-level DEMO BB requirements. Such requirements regard: the achievement of the needed Tritium Breeding Ratio to guarantee the fuel self-sufficiency in DEMO; the limitation of the tritium release towards the environment; the adoption of a structural material that minimizes the radioactive waste hazard; the selection of BB coolant thermal-hydraulic parameters in a way that maximize the cycle thermal efficiency [5]. In ITER, each TBM will be provided with dedicated auxiliary circuits. Together, TBM plus the related ancillary systems compose the TBS. The design and the functional characteristics of the different TBSs are dictated by DEMO operational conditions and selected requirements. For the HCPB, the design of such system is currently at a preliminary stage [6]. Referring to the WCLL, the TBS conceptual design was terminated in 2020 [7]. Its main ancillary systems are:

- Water Cooling System (WCS), whose thermal-hydraulic parameters are chosen in accordance with the DEMO requirement for power extraction.
- Coolant Purification System (CPS), for the purification of the primary water coolant.
- Lead-Lithium (PbLi) loop, for tritium breeding through PbLi circulation inside the TBM breeder units.
- Tritium Extraction System (TES), connected to the Lead-Lithium loop, consisting in a helium circuit for the tritium extraction from the PbLi flow.
- Tritium Accountancy System (TAS), whose function is the measurement of the tritium concentration in the PbLi flow, [8][9].
- Neutron Activation System (NAS), whose function is the monitoring of the local neutron flux and fluence inside the TBM set.

For what concerns the WCS, part of the activities to be performed consist in the thermal-hydraulic characterization and the verification of the capability to guarantee the TBM cooling function.

A similar concept for the WCLL-WCS is the water coolant circuit of the Japanese Water-Cooled Ceramic Breeder (WCCB) TBM concept. The conceptual design of this system was performed by National Institutes for Quantum and Radiological Science and Technology (QST) [10], and the activity for the preliminary design phase has already started.

The conceptual design of the WCS is presented and analyzed in this paper.

2 Conceptual design

2.1 Rationale

The relevancy of ITER WCLL TBM for DEMO BB has been recognized, in section 1, as one of the main objectives of the campaign [4] [5] [11]. It must be underlined that DEMO relevancy refers to the water thermodynamic conditions at the TBM, since the experimental programme will deal with the test of the BB reference concepts. Such thermodynamic conditions are inlet and outlet temperatures of 568 and 601 K, respectively, and average pressure of 15.5 MPa, [12].

DEMO BB foresees two sub-systems, i.e., the First Wall (FW) and the Breeder Zone (BZ). Each one is cooled by an independent Primary Heat Transfer System (PHTS). Instead, the reduced thermal power produced in the TBM set (near 700 kW) with respect to DEMO BB (1923 MW, [12]), allows to use a single water-cooling system for both the FW and the BZ. The WCS primary flow is computed considering the power input term and the required water thermodynamic conditions at TBM inlet/outlet.

The final heat sink for the WCLL TBM WCS is the ITER Component Cooling Water System (CCWS). With the aim to include an additional barrier between the contaminated primary water and the CCWS coolant, the WCLL-WCS is split in a Primary Loop (PL) and a Secondary Loop (SL). The first one contains contaminated water flowing outside the TBM-set and the second one avoids CCWS contamination with primary coolant, that may exceed the CCWS radioactive inventory limit (note that CCWS is a non-nuclear system). To simplify the WCLL-WCS management, liquid only condition is foreseen for the SL coolant instead of the two-phase fluid.

It is worth to emphasizing that electricity generation purpose is not foreseen for ITER and, thus, steam production is not required. CCWS provides low pressure water (around 0.8 MPa) at 304 K. Moreover, a further design constraint regards the CCWS water temperature increase, which must be limited to 10 K. Hence, there is a considerable difference between the average TBM temperature and the average CCWS temperature. To avoid an excessive temperature excursion, and thus thermal stresses, between the two sides of a single Heat eXchanger (HX), an economizer is foreseen in the middle of the WCS PL. This leads to the typical “eight” shape configuration for the primary cooling circuit. Therefore, a total of three HXs are considered for the whole WCS, namely:

- HX-0001: the economizer;
- HX-0002: the intermediate heat exchanger between PL and SL;
- HX-0003: the heat exchanger between WCS SL and CCWS.

The TBM is located on the high temperature side of the WCS PL and the water pumps on the low temperature branch, downward the HX-0002.

The WCS is installed in the ITER Tokamak building. Most of the equipment is in the level four TCWS Vault. The rest of the components, including the TBM, are placed in the level one Port Cell C16. Both locations are connected by means of Connection Pipes (CPs) arriving to the Port Cell #16 through the Vertical Shaft (VS). The different locations hosting the WCLL-TBM WCS are shown in [13]. An overview is offered by Figure 1.

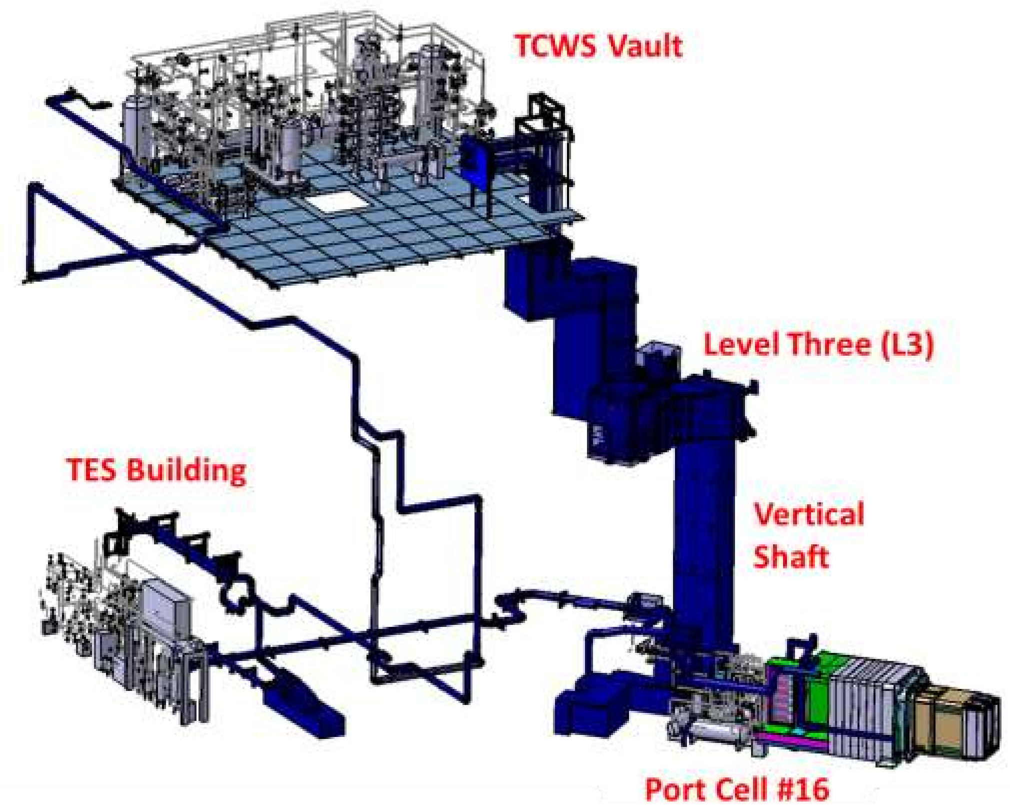

Figure 1. Location areas of the WCLL-TBS [13]

2.2 Process Flow Diagram

2.2.1 Primary Loop

A schematic view of the overall WCS is contained in Figure 2, showing all the essential components for the system operation. The rated TBM inlet flow is used to cool down both the FW and the BZ. A calibrated orifice (gross regulation) and a control valve (fine adjustments) are respectively located at the BZ and FW inlet lines to regulate the desired cooling flow rate through the two TBM areas. The regulation system ensures the proper refrigeration of all the TBM internal components.

The economizer limits below 100 K the average temperature difference between the WCS PL cold branch and the CCWS. This temperature difference is adopted as preliminary sizing criterion for the other two HXs (HX-0002 & HX-0003) as it affects their size and the technical feasibility. The economizing function is performed by a hairpin heat exchanger (HX-0001 in Figure 2). This technology is also used in the PWR nuclear power plants for small HX, as the Chemical Volume Control System (CVCS) HX. It preheats the water directed to the TBM with the hot one coming from the same component. The HX-0001 is sized to provide water to the TBM at the required thermodynamic conditions.

For the intermediate heat exchanger (HX-0002 in Figure 2) hairpin technology is also selected. This HX thermally couples WCS primary and secondary loops. The average temperature difference between the WCS PL cold branch and CCWS, mentioned above, is nearly equally distributed between the HX-0002 and the HX-0003. On the secondary side, the HX is equipped with a bypass line and a control valve (VC-0010 in Figure 2). This system allows to regulate the HX-0002 feedwater flow rate.

To increase the PL reliability and availability, the current design foresees two identical canned centrifugal water pumps, installed in parallel on the loop cold branch. During WCS Normal Operation State (NOS) only one of the two pumps is on; the other one remains in stand-by to be used as backup. The two circulators are designed to provide independently the rated flow rate for cooling the TBM. In Figure 2 the pump system is equivalently illustrated by a single pump component.

The Normal Operation State is characterized by a pulsed plasma regime with a burn phase followed by a dwell time. An electric heater (HT-0001 in Figure 2) is installed in the WCS PL in order to supply the deficiency of TBM thermal power during the dwell time, maintaining a constant temperature at the TBM inlet. During other WCS states, when no plasma pulses are foreseen, the electrical heater keeps the system temperature field as much as possible unmodified with respect to the one during NOS. The series of economizer and electrical heater is provided with a bypass line for temperature regulation at the TBM inlet. Bypass flow is set by means of two control valves: the former (VC-0001 in Figure 2), installed in the cold leg, downstream the electrical heater; the latter (VC-0006 in Figure 2), placed on the bypass line. This double-control valve system allows to regulate the bypass mass flow from zero up to the WCS primary loop rated flow.

The pressurizer (PRZ in Figure 2) system guarantees the pressure control function. It maintains WCS pressure at the required value independently on the temperature variations induced by the pulsed plasma operation or by other transient conditions. As a system operating at high pressure, the WCS PL must be equipped with a protection against low and over-pressure transients. The steam bubble pressurizer is connected to the PL hot leg by means of a surge line. The pressurizer is equipped with electric heaters and a spray line. The latter is connected to the PL cold leg. Spray flow rate is set by means of a control valve. These systems are installed to cope with under pressure (heaters) and overpressure (sprays) transients occurring during normal operating conditions and to limit pressure changes during transient conditions. In case of overpressure transients, if spray nozzles fail in reducing pressure, the PRZ is equipped with a Pilot Operated Relief Valve (PORV in Figure 2) and a Safety Relief Valve (SRV in Figure 2). They are both related to a relief line that connects the pressurizer to a Pressure Relief Tank (PRT in Figure 2), allowing the steam discharge. The PRT is a volume partially filled of water with a cover gas. The component is equipped with a pressure suppression system (spargers) and a rupture disk as a pressure release device.

A delay and a decay tank are installed at TBM outlet to reduce the $^{16}N/^{17}N$ content inside the WCS water.

2.2.2 Secondary Loop

The WCS secondary loop is foreseen to hydraulically disconnect WCS PL and CCWS. It avoids the CCWS water contamination, especially in case of HX tube rupture. The secondary loop is completely located in the TCWS Vault.

The hot water exiting the HX-0002 is led to the heat sink (HX-0003 in Figure 2), where it is cooled. Hairpin technology is also selected for the HX-0003. Thermal-hydraulic performances of the CCWS represent sizing constraints for the heat sink design. The heat sink is also equipped with a bypass line and a control valve (VC-0009 in Figure 2), to regulate feedwater flow rate.

The SL pump system design follows the one adopted for the primary loop. Two canned centrifugal water pumps are installed in parallel. Each one is sized to provide the SL rated flow independently.

The pressure control function is deputized to the pressurizer system. The main component is the steam bubble pressurizer, connected to the SL hot leg by means of a surge line. The tank (PRZ in Figure 2) is provided with the same equipment described for the analogous component in the primary loop: electric heaters, spray line, PORV and SRV. The relief line of these two valves is connected to the WCS PRT.

The CCWS pipeline section placed between the heat sink isolation valves (VG-0016 and VG-0018 in Figure 2) is protected against overpressure transients by a safety relief device (SRV in Figure 2). It connects this subsystem to the WCS PRT.

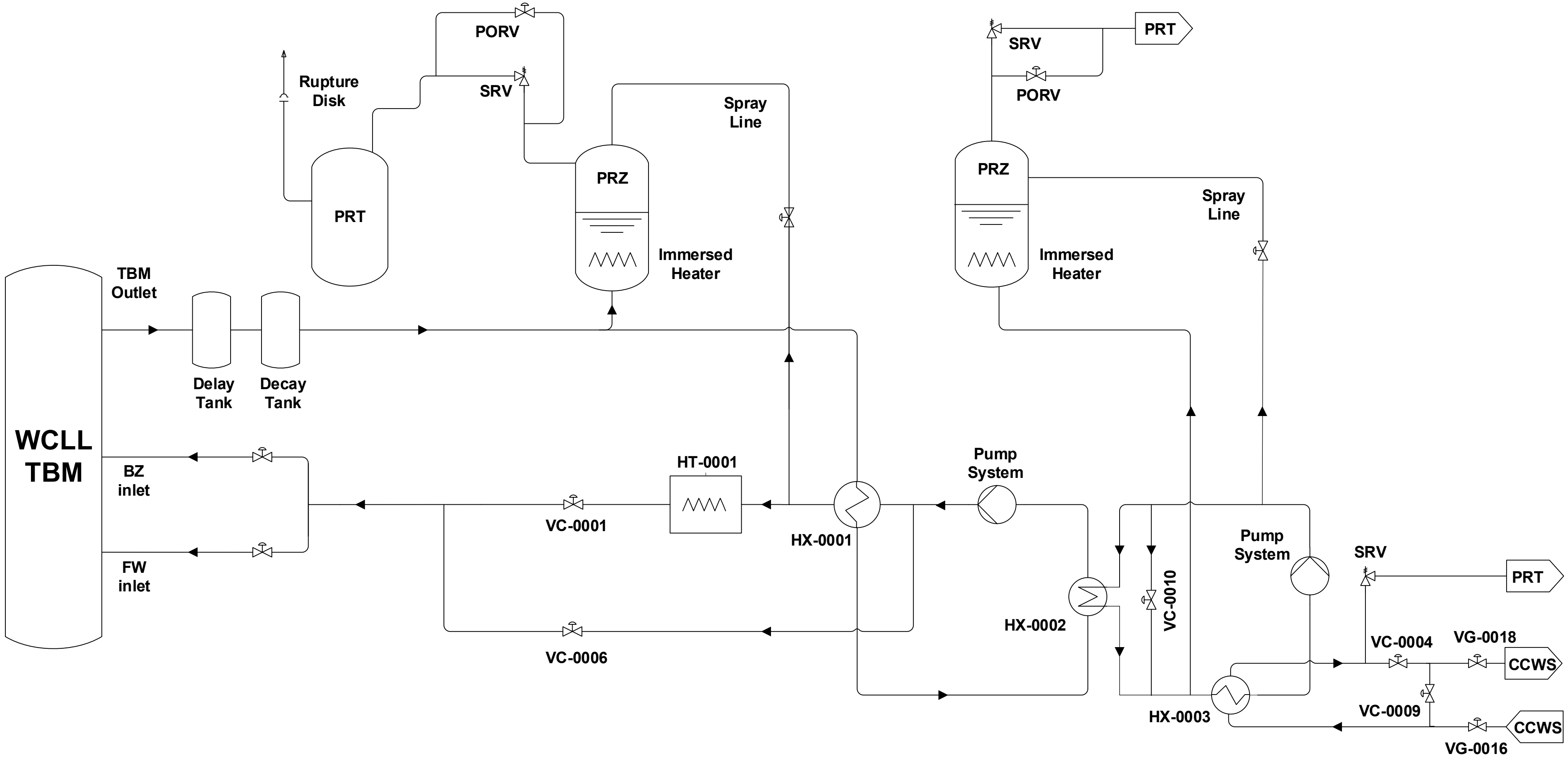

Figure 2. Schematic view of the WCLL-WCS circuit

2.3 Materials

The structural material used for the manufacturing of the WCS components (pressure vessels) and seamless piping is austenitic steel. Since there will be a certain amount of tritium that will permeate inside the WCS system, any material that could be a hydrogen getter shall be avoided. To respect this requirement, the austenitic steel AISI 316L is recommended as WCS reference material. Moreover, it is easy to weld and, as a stainless steel, it does not require a post-weld treatment (compared with equivalent ferritic steels that can be used at the same pressure and temperature). In addition, the material is widely used in the nuclear industry, which means that the technologies for manufacturing pressure vessels from this material are well established and documented. Thermal properties adopted for the austenitic steel in the WCS design are derived from ASME BPVC Section II [14].

For the thermal insulation of vessels, piping and components, preformed microporous insulation shells (filament reinforced pyrogenic silica) was selected [15]. The insulation thickness was sized with the requirement to keep external surface temperature below 323 K for safety purposes. The estimated overall heat losses are below 1% of the TBM rated power.

2.4 Heat exchangers

The hairpin design was selected for all the WCS HXs. The main advantage of this technology is the possibility to achieve high efficiency while having a very compact design with respect to a traditional Shell and Tubes. The hairpin is a proven technology for PWR reactors. It is used for small single-phase heat exchangers connected to the primary circuit, for example in the EPR CVCS circuit.

The heat exchanger layout consists in multiple straight horizontal fluid passages vertically arranged and linked by 180° curves. From the fluid-dynamic point of view, the hairpin heat exchanger is a pure counter-current device with hot fluid flowing inside the tube bundle and cold fluid within the shell. Heat transfer occurs only through the horizontal straight passages.

Tube sheets are foreseen at the beginning and at the end of each straight passage. Fluid exiting from the tube bundle is collected within the 180° curves and enters the following straight passage. Within the shell side, water flows from a straight passage to the next one through the inlet/outlet nozzles located slightly before the flanged connections. For constructive reasons, it is always recommended to use an even number of straight fluid passages. An example of the hairpin technology is presented in Figure 3, which shows the technical drawing of the HX-0002.

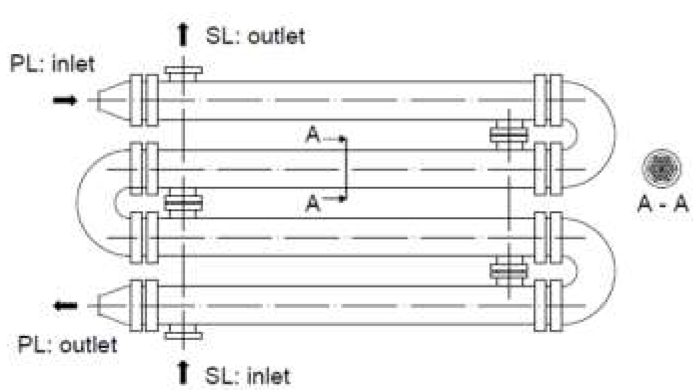

Figure 3. HX-0002: technical drawing

For the HX-0001 and the HX-0002, INCONEL is selected as tube material. It allows to reduce tube thickness maintaining nearly the same wall conductivity of the austenitic steel. The AISI 316L is used for the HX-0003 tubes. For what concerns the shell, austenitic steel is adopted for all the heat exchangers. Tube and shell steel thicknesses are preliminarily evaluated with ASME Sect. III NC [16].
The HXs design is performed considering the operation at End Of Life (EOL). Hence, fouling resistances are added to both internal and external tube surfaces and a 10% of tube plugging is taken into account in the calculation of the overall heat transfer surface. The reference internal and external fouling factors are conservatively taken from PWR design (typical commercial values), [17][18], without considering the reduced ITER operational life.

2.5 Piping and Pumps

The WCS piping diameter is sized to avoid excessive pressure drops in primary and secondary loops. Pipeline thickness is preliminarily evaluated following ASME Sect. III NC [16], while the component OD is selected from ASME B36.10M values [19].
For HX-0002 and HX-0003, the heat exchanger design pressure is considered up to the secondary side isolation valves. In this way, at least for a certain period, these sections of the secondary loop and CCWS can be operated with the valves closed. This conservative approach is not assumed for the rest of the correspondent systems.
Concerning the PC#16, due to the severe space constraints in this area, the main sizing criteria for all the components is the space allocation reduction. This is also the key design requirement for the pipelines going from the VS outlet to the TBM inlet. The pipeline size should be reduced as much as possible taking into account the compatibility of the increasing pressure drops with the maximum pumping capacity of the WCS PL. A sensitivity analysis was carried out to optimize this parameter.
This sizing reduction cannot be applied to the pipelines going from TBM outlet to VS inlet. In fact, in this WCS section, it is required to maintain enough residence time to reduce the N^{16} content in the contaminated water. The pipeline size reduction decreases the residence time in a way that might not be compensated by the delay/decay tanks.
Concerning the pumping system, the selected technology for both WCS PL and SL is the canned centrifugal pump. They are sized calculating the overall loop pressure drops and the required pumping power.

2.6 Pressure Control System

2.6.1 Primary Loop

WCS primary loop hot branch operates at thermodynamic conditions within the typical range of a PWR. For this reason, the pressure control system PWR design is adopted [20]. The main component of the system is the steam bubble pressurizer. As for PWR experience, the component volume is sized to accomplish the loop volume variations occurring during the maximum in-surge and out-surge transient conditions. The complete loss of heat source (plasma burn) and the complete loss of heat sink are selected as sizing criteria, respectively related to the out-surge and in-surge transients. The minimum pressurizer ID is calculated to avoid two-phase flow in the PORV valve throat section in case of water discharge during overpressure transients. The thickness is preliminarily evaluated with ASME Sect. III NC [16]. The pressure control function for WCS primary loop was developed according to the PWR experience, as recommended in [20].
As presented in section 2.2.1, the pressurizer is equipped with proportional electric heaters and a spray system. The proportional heaters are set to operate in a range of pressure around the WCS PL reference one. A varying input current, as a function of the pressure deviation signal, is supplied to the heater bank. Normally these heaters are energized at half current when pressure is at setpoint (no pressure error). The variable heaters will

be de-energized at the higher pressure setpoint and fully energized at the lower pressure setpoint. The spray line valve is regulated to modulate flow rate starting from a lower pressure setpoint up to a higher one correspondent to fully open valve. The operating range of this device is contained between the WCS PL reference pressure and the PORV valve opening setpoint. The spray system operates to prevent the opening of the pressurizer PORV and SRV. PORV and SRV actuation is required during overpressure transients in case spray nozzles fail in reducing pressure. PORV opening setpoint is lower than the SRV one to limit the number of challenges to the SRV. PORV and SRV area change rate and throat section are scaled from PWR design [20], based on the loop inventory and a safety margin.

In case of overpressure transient steam is discharged from the pressurizer to the PRT. The pressure suppression system of the PRT is based on immersed spargers that help in liquefy the steam coming from the pressurizer. The PRT is also provided with a rupture disk. The volume of this component is scaled from PWR design [20]. The scaling factor is based on the loop inventory and a safety margin and it is verified by the calculation of the condensing capacity in case of a discharge for a complete pulse phase.

2.6.2 Secondary Loop

The secondary loop pressurizer system is designed following the main outlines discussed for the WCS PL. The main difference is the procedure for sizing the steam bubble pressurizer. The method described for the analogous component of the WCS primary loop is not applicable in this case. Operative conditions of the WCS secondary loop are different from the PWR ones. The strategy adopted is to scale the SL PRZ size from the PL PRZ one. The scaling factor is evaluated from the ratio between loop inventories. In addition, a safety margin is applied. The pressurizer equipment is sized by performing numerical simulations concerning operational transients involving the WCS secondary loop. The discharge volume for the SL PRZ is the WCS PRT.

2.7 Temperature Control System

The solution adopted for the electrical heater is a vessel equipped with heating elements immersed in water. The construction is like the one of a Shell and Tubes heat exchanger with the tubes replaced by hairpin Heating Rods (HRs). The component length is mainly given by the length of the HRs and the size of the head holding the electric contacts. The sizing power of such heat exchanger is discussed in paragraph 3.2.1. The HRs selected for the WCS electric heater design are taken from [21]. Austenitic steel is adopted as shell material. Since the component layout is similar to a Shell and Tubes heat exchanger, the Kern methodology is employed to assess thermal-hydraulic performances, such as pressure drops and Heat Transfer Coefficient (HTC) [22].

The requirement of the Temperature Control system is to provide water to the TBM at constant temperature over the pulsed regime. This parameter can deviate from the reference value mainly for two reasons. The first one is related to the design approach. Heat exchangers are designed to match nominal power in EOL operation. Hence, under Beginning Of Life (BOL) conditions, the components result oversized, modifying the WCS temperature field. In order to meet required TBM inlet conditions in both EOL and BOL, the mass flow rate across the shell side of the heat exchangers must be regulated. The modulation is obtained with the bypass lines and the control valves. The second deviation derives from the pulsed operation, leading to fluctuations of the water temperature at TBM inlet. In this case, the regulation is in charge of the electrical heater and it is obtained by tuning the electric power supplied.

The regulation of the heat exchanger performances is linked to the temperature measurement at the tube side (hot fluid) outlet. When the measured temperature decreases below the reference setpoint (i.e., the exchanged power is too high), the bypass valve starts to open, and part of the shell side (cold fluid) flow rate is redirected towards the bypass line. Therefore, heat exchange decreases and temperature at tube side outlet returns to

match the reference setpoint. The economizer control system intervenes, under BOL, to compensate the component higher performances and, during NOS, to absorb the TBM outlet temperature fluctuations due to pulsed regime. Instead, the HX-0002 and heat sink control systems intervene only under BOL to modulate the performances of the correspondent heat exchangers. In fact, during NOS, the temperature fluctuations disappear downward the economizer, as widely discussed in section 3.2.1.
The regulation of the power supplied by the electric heater is based on the acquisition of the TBM inlet temperature. If, for any reason, it drops below the setpoint (568 K), the electrical heater comes into operation, supplying the deficit and restoring the required inlet temperature. A Proportional/Integral (PI) control system continuously regulates the HT-0001 power.

3 Thermal-hydraulic analysis

The computational activity discussed in this paper consists in a preliminary Thermal-Hydraulic (TH) analysis of the WCLL-TBS WCS. The aim is to assess system capabilities under the normal operational state and selected abnormal scenarios. Among the WCS goals, the cooling system must guarantee: required conditions at TBM inlet; enough margin from the PbLi freezing temperature in every part of the PbLi loop (included the section inside TBM). To carry out a complete analysis, the thermal-hydraulic model includes WCS, TBM-box and PbLi loop.

The expected outcomes of the analysis were the following:

- Pressure and temperature fields.
- Overall pressure drops in NOS and related pump design.
- Margin from PbLi freezing temperature in selected critical points (inside TBM, Cold Trap outlet, etc.).
- Thermal balance.
- Capability of the WCS design to overcome selected abnormal conditions.

The analyses was carried out with a modified version of the RELAP5 Mod3.3 system code [23], developed at the Department of Astronautical, Electrical and Energy Engineering (DIAEE) of “Sapienza” University of Rome [24], in collaboration with the Italian National Agency for New Technologies, Energy and Sustainable Economic Development (ENEA) [1]. New features were implemented to improve the capability of the code for fusion reactors application. The ones relevant for the current simulation activity are: PbLi working fluid thermophysical properties in according with [25]; Seban-Shimazaki [26] correlation to simulate liquid metal heat transfer coefficient within circular tubes or plates.

3.1 Description of the thermal-hydraulic model

The thermal-hydraulic model was developed at (DIAEE), improving the nodalization scheme used for the preliminary assessment of the previous version of WCS [27].

The whole thermal-hydraulic model is presented in Figure 4 and Figure 5. The main features of the input deck are the following:

- Geometrical data of all the pipelines and components keep the reference design;
- Actual elevations are maintained for any component;
- The ratio between the length of two adjacent control volumes (CVs) is kept below 1.25.

Figure 4 shows the modelling of WCS, CCWS and PbLi. For space limitations, the figure does not represent actual elevations of the model, as well as of the design. It aims to provide a schematic view of the nodalization, presenting the qualitative elevation differences of the main components and their connections. The relevant components are depicted in grey for the WCS primary system, in light blue for the WCS secondary loop, in green for the CCWS and in orange for the PbLi. They are identified by the name and the component number (following the "#"). The pipelines, simulated with several pipe components, are represented with black lines, identifying some relevant connections, such as valves, pumps, and time-dependent junctions (black arrows). Time-dependent volumes are used to set inlet and outlet boundary conditions for specific components. They are represented with a peculiar symbol (a circle inside a square).

Hot water exits TBM and flows through the pipe forest (component #300 in Figure 4), placed in Port Cell 16 (see left corner at the bottom of Figure 4). It connects TBM outlet with the first delay tank (#302), located within the Pipe Forest. Exiting the tank, the pipeline installed within the Vertical Shaft leads hot water first to the second delay tank (#312), at level three (L3) and then to the TCWS Vault area. The pipelines are modelled with several pipe components, keeping design features. Each delay tank is modelled with a vertical pipe component, maintaining the nominal inventory.

Within the TCWS Vault, water is headed to the economizer (HX-0001). Hot water flows across the tubes, pre-heating the water flowing through the shell side. Inlet and outlet plena are modelled with two branch components, maintaining the nominal inventory. The whole tube bundle is collapsed in a single equivalent pipe component. From the hydraulic point of view, this pipe is characterized by the overall flow area, the length and the hydraulic diameter of a single tube. This modelling approach allows to keep the actual inventory and the hydraulic features of the bundle. The flow area is affected by the operative conditions. As presented in section 2.4, the HXs are designed under EOL condition. The goal of the thermal-hydraulic analysis is to verify the WCS performances in both EOL and BOL. From the hydraulic point of view, the main difference is related to the total flow area of the tube bundle. Due to the postulated plugging, under EOL operation the flow area is reduced by 10%. The HX shell side is modelled with a pipe component. It is characterized by the nominal length and the total flow area that is calculated as the difference between inner area of the shell and the area occupied by the tubes. In this case, flow area is not affected by the operative conditions since the effect of the postulated fouling is negligible in terms of flow area blockage. Several heat structures (HSs) simulate the heat exchange between the two sides. In Figure 4, the yellow portion between hydrodynamic components represents passive heat structures for the heat transfer. The heat transfer surface kept the nominal value. This parameter is affected by operating conditions. Under EOL it is reduced by 10% due to the postulated plugging. Regarding the fouling, fouling factors are calculated on the basis of the reference data and applied on both the sides, increasing the heat transfer resistance. The modelling approach described above is applied to each heat exchanger belonging to the Water-Cooling System.

Downward the HX-0002, only one of the two primary coolant pumps is modelled. It is simulated with a pump component (#337), assuming the reference parameters of the selected pump. A PI controller is applied to control pump velocity, setting the mass flow rate setpoint. The same modelling approach is adopted for the pump system of the secondary loop.

The electric heater is modelled with a pipe component. The goal of the modelling approach is to keep the heat transfer capability (i.e., the HTC) and the water inventory of the component. For this purpose, the equivalent flow area of the pipe component is calculated according to the Kern methodology [22]. The hydraulic length of the component is evaluated to maintain the actual inventory of the heater. This modelling approach results in a longer component. From a hydrodynamic point of view, this discrepancy is negligible compared to the overall length of the primary cooling system. Regarding the heat transfer surface, the nominal value is maintained by applying specific geometrical factors to the heat structures simulating the power supplied by HRs. These active heat structures are represented by a red rectangle in Figure 4. The supplied power is provided by a control variable. The temperature of the control volume at the outlet of the TCWS Vault is compared with the reference setpoint. An enthalpy error signal is produced, and it is multiplied by the cold leg mass flow rate (acquired just before the control volume). A value of power unbalance is produced and scaled adopting a PI controller, where a minimum value equal to zero is imposed. The resulting signal is divided among the heat structures simulating the heating rods.

Exiting the electric heater, the cooling water flows through the descending vertical shaft reaching the Port Cell 16. The TBM is fed by means of two conduits which provide water to the FW and the BZ systems.

The pressurizer allows to keep desired primary pressure. The PRZ is modelled with a vertical pipe component, composed of seven control volumes. The first and the last CVs simulate the heads of the tank. The overall water inventory is kept by calibrating the flow area of these two CVs. The overall height of the component is respected. The PRZ electrical heater is simulated with an active heat structure connected to the second CV from the bottom. Thermal power supplied to the water is obtained from a general table and it is a function of the pressure deviation signal (computed by a control variable). The PRZ is coupled to the primary loop using a surge line (#402), connected to the hot leg, and a spray line (#406 and #408), connected to the cold line. The flow rate through the spray line is regulated by a time-dependent junction (#407), setting the injected value as function of the pressure deviation signal. A trip disables the time-dependent junction in case of accidental scenario (for example loss of flow accident). In case of abnormal operation, if spray nozzles are supposed to fail or are disabled, PRZ discharges steam firstly through the PORV (#410), and then through the SRV (#412). The two valves are modelled with motor valve components connected to two time-dependent volumes that reproduce the pressure relief tank environment. Opening and closure of these components are regulated by control trips, calibrated with design setpoints. The PRZ modelling approach is also adopted for the secondary pressurizer system.

As presented in section 2.7, the HXs performances are regulated by means of bypass lines. The HX-0001/HT-0001 bypass line is modelled with a pipe component (#437) connecting upward the HX-0001 and downward the HT-0001. The pipeline is equipped with a control valve, simulated with a servo valve component (#438). Openings and closures are regulated by a control variable. The temperature reading at the Tube-side outlet is compared with the setpoint. An error signal is produced and scaled using a PI controller which operates in the range 0-1. The resulting signal is imposed as valve position for the component #437. This control logic is also adopted for the heat exchange regulation of HX-0002 and HX-0003. Concerning the HX-0003, the signal from the PI controller is assumed as valve position for component #518, while valve #510 operates oppositely than #518.

As far as the CCWS connection is concerned, only the portion within the TCWS Vault is modelled. Inlet temperature and outlet pressure of the coolant are set by two time-dependent volumes. A time-dependent junction imposes the feedwater mass flow rate. The loop is equipped with a safety valve, modelled with a motor valve component (#539). Valve actuation is regulated by a control trip, calibrated on the basis of the design setpoints. When the safety valve opens, the coolant is discharged into the PRT, reproduced with a time-dependent volume.

The heat losses towards the environment are modelled for all the components belonging to the WCS. Thermal properties of the structural material and the thermal insulator are set as input in the model. Pipes and insulator thicknesses are imposed according to nominal data. On the outside, HTC and environment air temperature are imposed as boundary conditions.

The overall pressure drops of the loops are computed by the code. The geometry and the number of bends are imposed according to the design. Calibrated K-loss coefficients are introduced to simulate local pressure drops: abrupt area changes, bends, filters, valves and grids. K-coefficients are calculated by using formulas derived from [28].

Although the PbLi loop is not directly involved in the WCS design, it can affect its operations, since the WCS must ensure that metal freezing is avoided in all operational states. For this reason, and to provide useful information to the PbLi design team, a detailed thermal-hydraulic model of the PbLi loop has been developed and coupled to the ITER WCLL modelling. The nodalization scheme consists of the pipelines, represented by black lines in Figure 4, and of the main components, depicted in orange.

Exiting the TBM, PbLi flows through the pipe forest, which leads the liquid metal from the Port Interspace to the Ancillary Equipment Unit Area. The PbLi enters the electrical heater (#611), which is in charge of increasing the liquid metal temperature to the operational value of the Tritium Extraction Unit (TEU). No information has been provided regarding the heater geometry. For the scope of this activity, it is preliminarily considered as a portion of the pipeline, where PbLi is warmed up by heating cables. Active heat structures supply power to the liquid metal. The thermal power is evaluated at each time step with a control variable, following the same control logic adopted for the WCS HT-0001. This approach allows to absorb temperature oscillations due to reactor pulsed operation and to provide PbLi with a constant temperature at TEU inlet.

The Tritium Extraction Unit is preliminary modelled with a descending vertical pipe, keeping actual inventory and elevation change (#611). Downward, the water-air heat exchanger cools-down the PbLi up to the storage tank operating temperature. According to the design, the cooler is simulated with a pipe component. Active heat structures removed the needed power (see blue rectangle in Figure 4). The thermal power is regulated with a PI controller. After that, part of the flow rate is directly driven towards the storage tank. The rest of the flow is directed to the Cold Trap (CT), which has in charge the PbLi purification. During NOS, a fraction of the total PbLi flow rate is continuously headed to the CT for alloy purification. To fulfil this scope, the component is cooled by an air flow, furtherly reducing the PbLi temperature. The unit is modelled with a pipe (#630), following the characteristic geometry of the component. The liquid metal inventory is maintained. The PbLi cooling is simulated by removing a constant thermal power with an active heat structure.

The storage tank is modelled with three vertical parallel pipes (#638, #639 and #640), connected with multiple cross junctions. This modelling approach allows to reproduce buoyancy within the large volume. The cover gas pressure is set with a time-dependent volume connected to the upper part of the pool. A time-dependent junction (#644) reproduces the pump. It fixes the overall mass flow rate through the PbLi loop.

Several heat structures reproduce the heat losses related to each component of the liquid metal loop. For the external conditions, the same boundaries used for the WCS are applied. The heat losses are a crucial aspect for the PbLi loop, especially downwards the CT, since metal freezing must be avoided and PbLi must be provided at TBM inlet with the required thermodynamic conditions. For this purpose, active heat structures compensate the heat losses that occur through the walls of the storage tank and of the pipelines connecting the tank and the TBM inlet. The necessary thermal power is managed by using a PI controller.

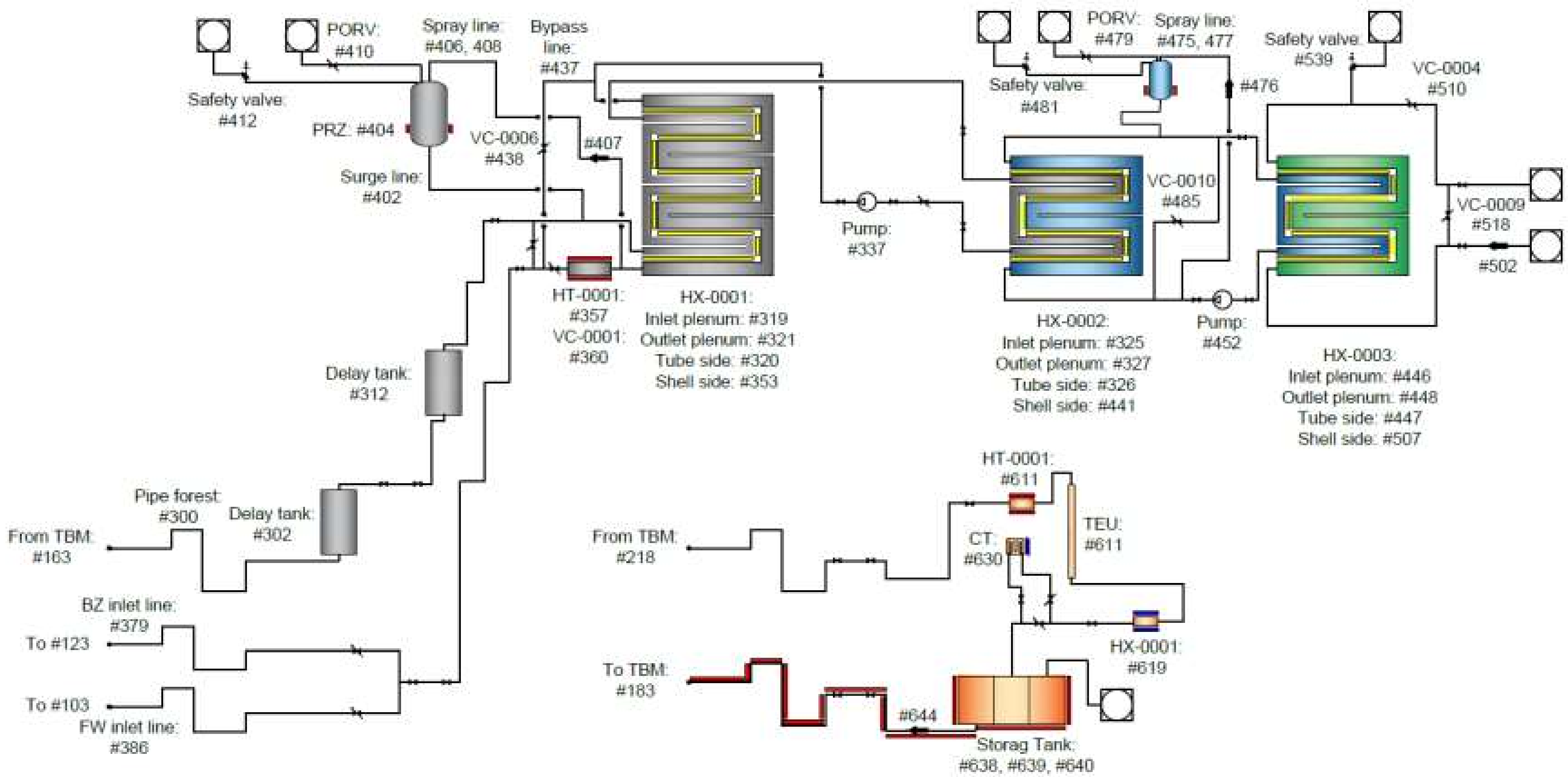

Figure 4. Nodalization scheme: WCS, CCWS and PbLi loop

Figure 5 shows the TBM nodalization scheme. The TBM reference geometry is derived from [29]. On the back of the BZ, four Back Plates (BPs) define four manifolds:

- FW inlet manifold: responsible for the water inlet of FW channels;
- BZ inlet manifold: responsible for the water inlet of Double Wall Tubes (DWTs);
- Water outlet manifold: responsible for the water outlet of DWTs and FW channels;
- PbLi manifold: responsible for the inlet/outlet of the PbLi within the Breeder Units (BUs).

The three manifolds belonging to the water system are modelled with three vertical pipes (one per each manifold), composed of 16 CVs. The inventory of each manifold is kept by calibrating the flow area. The upper and lower CVs of the FW manifold (#105) are connected to the inlet of the FW channels, collapsed in two equivalent pipes (#105 and #161): one for the descending and one for the ascending channels. At the outlet, the two FW equivalent channels are connected to the outlet manifold (#161). An overall number of 168 heat structures simulates the heat exchange within the FW:

- 32 HSs for the surface directly facing the plasma: the heat flux from the plasma and the power deposited in the EUROFER thickness are imposed as boundary conditions. In addition, thermal conduction between adjacent portion of the FW is taken into account using several control variables, which evaluates the heat transfer on the basis of the structural temperatures;
- 16 HSs for the radial-toroidal segments of the FW component: the power deposited in the structure is imposed as an internal power source;
- 24 HS for the EUROFER ribs between FW channels: internal power source is set as boundary condition;
- 96 HS for the heat exchange between FW channels and PbLi BUs: internal power source is imposed as a boundary condition.

The BZ inlet manifold (#125) feeds the DWTs. The DWTs are collapsed in 16 equivalent pipes, connected at each level of the inlet and outlet manifolds. An overall number of 288 heat structures simulates the heat exchange within the BZ.

The PbLi manifold is simulated with four vertical pipes: two for BUs inlet (#187 and #204) and two for BUs outlet (#197 and #214). The overall inventory is maintained. The BUs are modelled with 16 pipe components. An overall number of 208 heat structures reproduces the heat exchange within the PbLi area.

In addition, the heat exchange through the BPs is simulated with an overall number of 136 HSs.

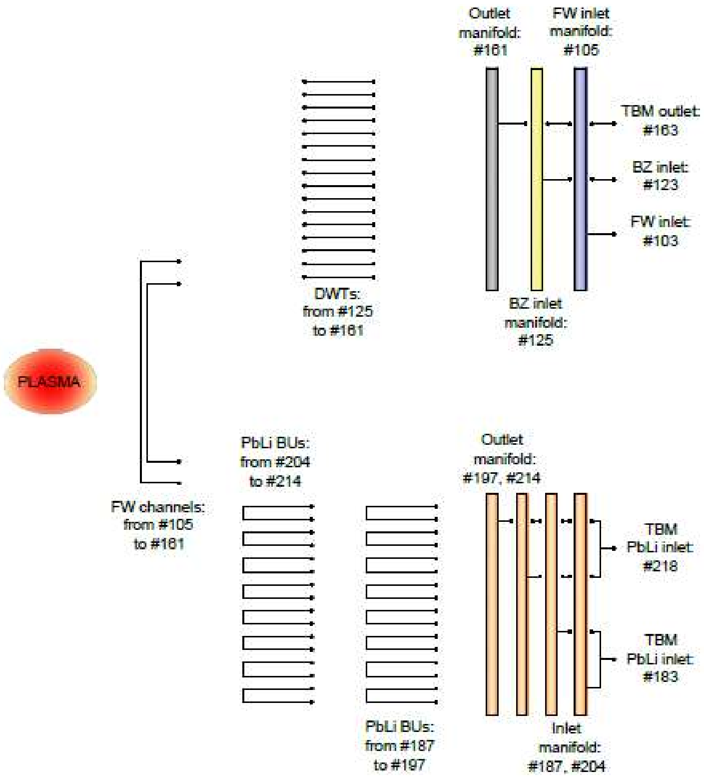

Figure 5. Nodalization scheme: TBM

3.2 Computational activity

This section analyses the main results of the computational activity. It is divided in two subsections:

- Section 3.2.1 summarizes the assessment of the WCS performances under the Normal Operation State, highlighting similarities and differences between BOL and EOL.
- Section 3.2.2 contains the transient analysis performed to support the system design. The Loss of Heat Sink (LOHS) due to a loss of flow in the CCWS has been selected to show the WCS layout capability to overwhelm abnormal conditions.

Also, the loss of flow in the secondary loop has been investigated. Simulation results are similar to the ones of the LOHS in the CCWS, then it is not presented since enveloped by the other transient.

The LOHS simulation has been repeated assuming four values for the time step (5.0E-03, 3.0E-03, 2.0E-03 and 1.0E-03). The time step sensitivity has highlighted the independence of the simulation outcomes from this parameter.

3.2.1 Normal Operation State

In order to assess the capability of the thermal-hydraulic model to simulate WCS operation, steady state calculations, involving BOL and EOL conditions, have been carried out. The analyses reproduce the full plasma power state. Then, this state is set as initial condition for the transient analyses simulating the overall NOS pulsed regime.

A total thermal power of 723.16 kW is supplied as boundary condition, distributed among the TBM heat structures presented in section 3.1. The mass flow rates through the CCWS and the PbLi loop are imposed as constant boundary conditions.

Table 1 summarizes the most relevant outcomes of the steady state calculations, comparing BOL and EOL results with the nominal values. Parameters indicated with "(Imp.)" are set as boundary conditions. The main requirements are the fixed conditions at the TBM inlet: 3.74 kg/s at 568.15 K for the WCS PL water and 0.65 kg/s at 568.15 K at for the PbLi. As shown in Table 1, WCS respects the requirements in both BOL and EOL. The main relevant differences between the two operative conditions are the flow rate through the shell side of the heat exchangers. As expected, the temperature control system intervenes to modulate the mass flow rate, regulating the power exchange to match the reference values. HX-0001 preheats cold coolant directed to the TBM using hot water coming from the TBM itself. It must be underlined that HX-0001 does not contribute to the energy balance of the WCS PL, since its power is transferred from a branch to another, within the circuit itself. Downward the HX-0001, the electric heater supplies power to compensate heat losses, which are estimated to be around 11 kW for the WCS Primary Loop (PL). The difference in terms of HT-0001 power is due to the power removed from the WCS (through HX-0003), slightly higher at EOL. This difference is due to the control system operation. Concerning the pressure drops, slight differences are observed between BOL and EOL. They derive from HXs tube plugging.

Regarding the PbLi loop, for the scope of this activity, differences between BOL and EOL are not implemented in the liquid metal system (for example, flow blockage in the cooler). For this reason, the same results are presented for the two operative conditions. The TBM inlet requirements are respected and a satisfactory margin from the PbLi freezing is ensured in the whole system. The overall loop pressure drops are strongly affected by the magnetohydrodynamic (MHD) effects, mostly present near the TBM where the magnetic field is relevant [30]. For this, such evaluation is not reported in the paper.

Table 1. Full plasma steady state calculation: main results

System	Parameter	Unit	Nominal value	BOL	EOL
WCS PL	Total mass flow	kg/s	3.74	3.74	3.74
	HX-0001 mass flow rate (shell-side)	kg/s	--	3.45	3.74
	TBM Outlet T	K	601.15	600.82	600.82
	HX-0001 Outlet T (tube-side)	K	430.18	429.78	430.99
	HX-0002 Outlet T (tube-side)	K	384.55	384.53	384.48
	TBM Inlet T	K	568.15	568.08	568.08
	Pump head	Pa	--	7.73E+05	7.86E+05
WCS SL	Total mass flow	kg/s	4.3	4.3	4.3
	HX-0002 mass flow rate (shell-side)	kg/s	--	2.7	4.1
	HX-0003 Inlet T (tube-side)	K	378	378.07	378.32
	HX-0003 Outlet T (tube-side)	K	338	337.91	337.41
	Pump head	Pa	--	1.16E+05	1.39E+05
CCWS	Total mass flow (Imp.)	kg/s	17.3	17.3	17.3
	HX-0003 mass flow rate (shell-side)	kg/s	--	5.41	15.12
	Outlet T	K	314.15	314.17	314.36
WCS	TBM power to WCS	kW	--	718.48	718.51
	HX-0001 power	kW	3112.5	3104.1	3084.7
	HX-0002 power	kW	722.8	723.35	736.09

	HX-0003 power	kW	722.8	724.89	738.23
	HT-0001 power	kW	--	11.96	24.58
PbLi loop	Total mass flow (Imp.)	kg/s	0.65	0.65	
	TBM Outlet T	K	--	604.03	
	TBM Inlet T	K	568.15	568.15	
PbLi loop	TBM power to PbLi	kW	--	4.42	
	HX-0001 power	kW	--	17.99	
	HT-0001 power	kW	--	15.48	
	Heating cables: F1LP-P-0001 & F1LP-P-0003	kW	--	0.81	
	Heating cables: TA-0002	kW	--	1.23	

Steady state results have been imposed as boundary conditions for the transient analysis aimed at investigating the WCS behavior during the overall NOS pulsed regime. System thermal-hydraulics is analyzed in both BOL and EOL.

The pulsed plasma regime is characterized by a full plasma power kept for 450 s. After this flat-top condition, power is ramped down in 200 s. The dwell time between two consecutive plasma pulses is 1090 s. Finally, power ramp-up lasts 60 s [27]. In the following plots, the pulse phase is characterized by a white background while dwell phase by a grey background.

The transient analyses start with the flat-top condition (see Table 1). The simulation time is set to 14000 s, corresponding to eight complete cycles of pulsed regime. WCS pumps (in both primary and secondary loops) work at nominal velocity over the whole simulation, keeping almost constant primary and secondary flow rates (relevant for DEMO operation [27]). CCWS inlet conditions (i.e., temperature and feedwater flow rate) and outlet pressure are kept constant.

Figure 6 shows water temperature at inlet and outlet sections of the TBM. The requirements at the TBM inlet are verified (in both BOL and EOL): temperature control system guarantees almost constant inlet temperature (around 568 K), while the mass flow rate is ensured by the pump. Fluctuations in the TBM inlet temperature, due to the pulsed regime, are limited to +/- 3 K. This value is considered admissible for the system operation. At the TBM outlet, temperature assumes values in the range of 568 – 602 K, following the pulsed regime. The most relevant exchanged powers referring to WCS are presented in Figure 7. It compares TBM power delivered to the WCS, heat removed in HX-0002 and HT-0001 supplied power. The power delivered from the TBM to the WCS changes in the range of 8.5 – 680 kW provoking the temperature fluctuations observed in Figure 6. These oscillations at TBM outlet are absorbed by the temperature control system, modulating the coolant flow rate across the HX-0001 shell side. In the WCS section between HX-0001 tube side outlet and HX-0001 shell side inlet, quasi-steady state conditions are maintained over the whole operation. The temperature control system regulates HX-0002 power to the almost constant power of 720 kW. At BOL operation, when the HX-0002 is oversized, around 1.6 kg/s bypasses the HX-0002 shell side (nearly 40% of the nominal secondary loop mass flow rate). The electric heater has in charge to compensate power unbalance of the system. HT-0001 power is regulated by the temperature control system. It assumes an opposite trend than the TBM power, working in the range of 80 – 699 kW.

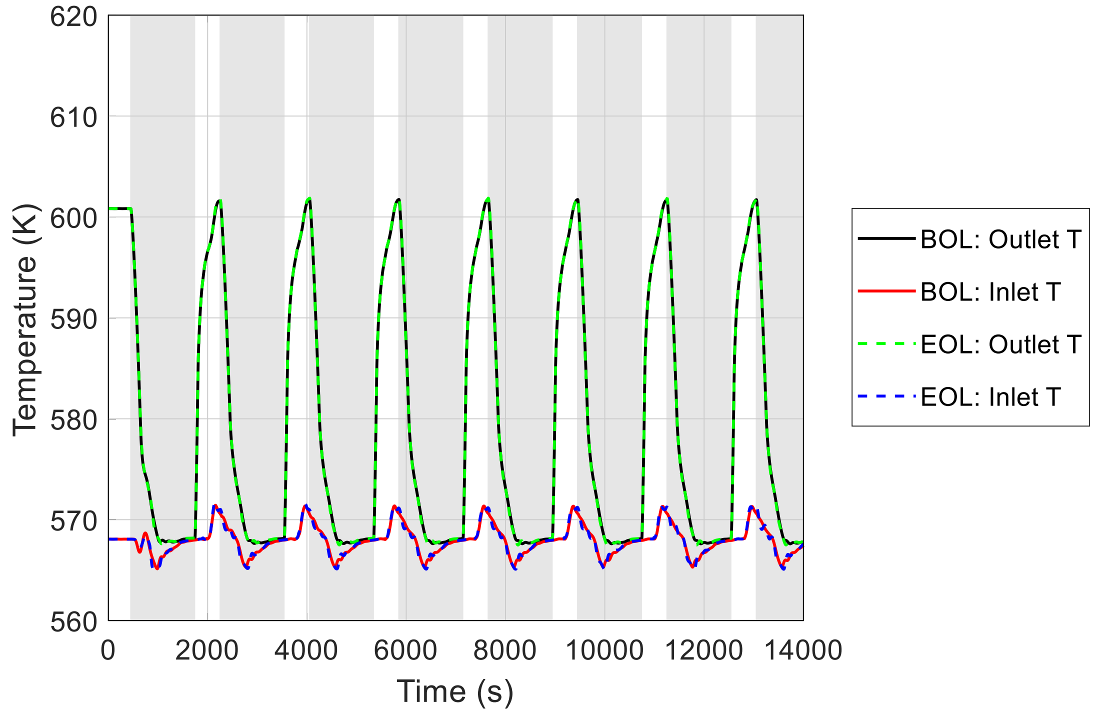

Figure 6. WCS: TBM inlet and outlet temperatures

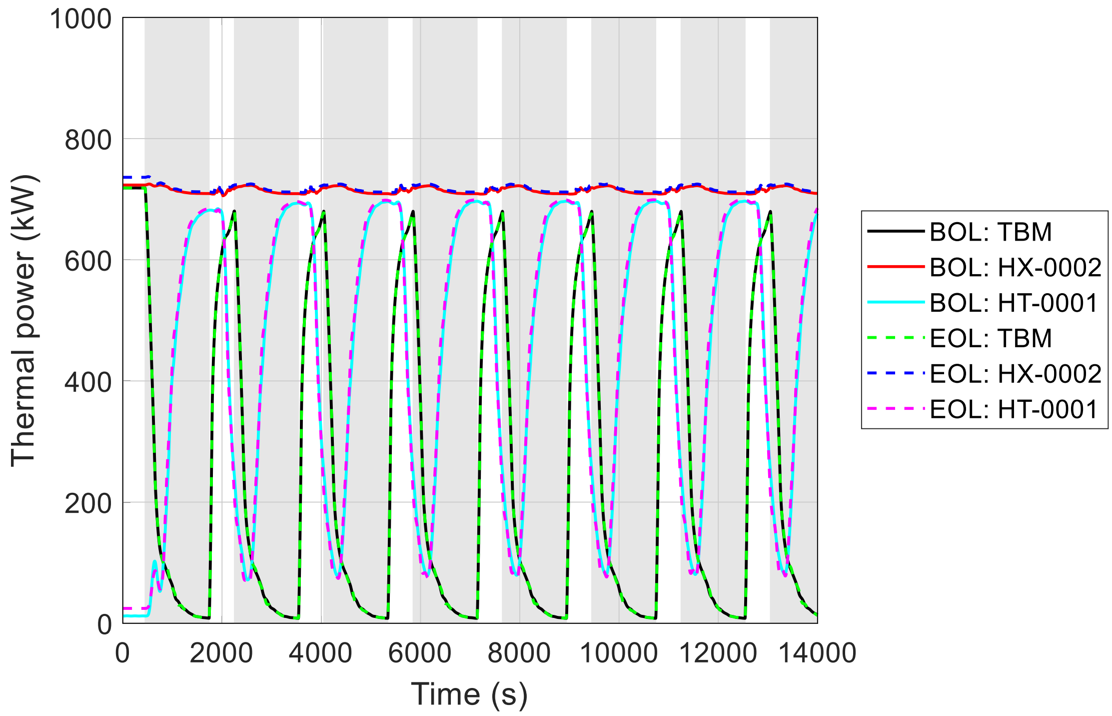

Figure 7 Thermal power: TBM, HX-0002, HT-0001

WCS Secondary Loop (SL) and CCWS work at quasi-steady state conditions. Bypass flow rates are regulated by the temperature control system to ensure the reference heat exchange and to guarantee the required water temperature at the CCWS return.

Concerning the PbLi loop, TBM inlet conditions are verified. At the TBM outlet, PbLi temperature assumes a fluctuation trend typical of the pulsed regime. Oscillations are absorbed by the electric heater, whose power is regulated by the temperature control system to ensure the operative temperature of 723 K at the TEU inlet. Downstream the electric heater, the system works at quasi-steady state conditions. The coldest region of the loop is the CT outlet pipe, where PbLi reaches 526 K. The margin from the freezing point is kept at 16 degrees. In the following design phase, the appropriateness of this margin will be evaluated. If the current value is considered too low, heating cables will be activated to increase the minimum temperature reached in the PbLi loop.

3.2.2 WCS performance during degraded operations - LOHS

In order to assess and verify the WCS design, an abnormal scenario has been selected and investigated. The aim is to assess the WCS capabilities under degraded conditions and to verify if the standard control strategies without any external action are capable to maintain the TBM cooling function for an entire ITER pulse. This last condition allows to avoid the triggering of the fast plasma shutdown system (FPSS), demonstrating that a minor incident in the WCS does not interfere with the ITER global operation. The transient considered consist in the LOHS (loss of flow in the CCWS). The worst operative condition is supposed to be the EOL, since plugging and fouling limit the heat exchange. For this reason, NOS at EOL is imposed as an initial condition for both the transient analyses.

The Postulated Initiating Event (PIE, t = 0 s) occurs at the beginning of the flat-top condition. It represents the worst scenario since the plasma termination is supposed to be triggered only at the end of the pulse. In the next plots, this phase is represented with the red background. The plasma termination occurs at 450 s, after which TBM power decreases to the decay heat value. The PIE consists in the blockage of the CCWS circulator (i.e. the time-dependent junction #502 is turned off). The current RELAP5 model does not include the overall CCWS system, but only its section located in TCWS Vault. Time dependent volumes and junctions are used to simulate the CCWS inlet/outlet. This modelling approach does not allow to model the natural circulation flow establishing in CCWS after the pump stop. For this, conservatively, to the mass flow rate through the time-dependent junction #502 has been imposed a decreasing trend from nominal value to zero in 1 second.

Furthermore, the pressure at CCWS outlet is imposed as boundary condition. This is acceptable for simulations involving operational states, when the system reference pressure is imposed at the outlet and no pressure transients are expected. Instead, for these scenarios, such hypothesis could impact the computed results. In fact, the outlet pressure is fixed for all the calculation and the pressure transient is not simulated in the CCWS section considered. Consequently, the HX-0003 heat exchange performances could be altered during the overall transient evolution. For this reason, the isolation valve located at the outlet of HX-0003 CCWS side (VG-0018) has been conservatively closed in the simulation. Actually, this action is not foreseen in the management of such scenario. Although, in this way, even if the transient simulated is more conservative, the simulation outcomes are reliable to assess the WCS TH performances during degraded conditions. This second closure occurs 5 s after the PIE.

WCS primary loop is kept in normal operation over the whole transient: the control system ensures the temperature and pressure regulation and the primary pump continues to operate. On the secondary loop, in order to avoid cavitation in the component, SL pump is disabled when the inlet water temperature rises above 10 degrees below the saturation temperature at the operative pressure. A control variable regulates the operation of the pump component #452. SL PRZ sprays are disabled when the pump head decreases to 80% of the nominal value. The PbLi is kept in operation over the whole transient. No further actions are foreseen up to the end of the simulation (8600 s).

Figure 8 presents the HX-0003 feeding mass flow rate. At 0 s the PIE occurs, and the flow rate decreases to 0 in 1 s. Water temperature starts to increase (see red line in Figure 9) and, following the closure of the outlet isolation valve, pressure within the isolated section of the CCWS rises. The first opening of the safety valve (#539 in Figure 4) occurs after 12 s from the PIE, and it is followed by repeated opening and closing cycles (Figure 10). Figure 11 shows the power exchanged in HX-0002 and HX-0003. HX-0003 power drops to 93 kW in 2 s. Then, the reduction rate decreases, due to the safety valve openings. The minimum value of the HX-0003 power in the first phase of the transient is reached at 720 s (around 50 kW). At this time, water within the HX-0003 reaches saturated conditions and starts to boil, increasing HX-0003 power (see the first fluctuations of the red line in Figure 11). Steam production leads to a further increase in the frequency of the safety valve opening/closing cycle.

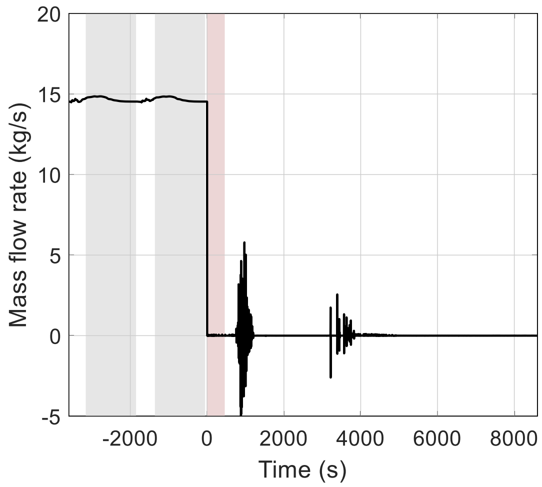

Figure 8. CCWS: HX-0003 mass flow rate

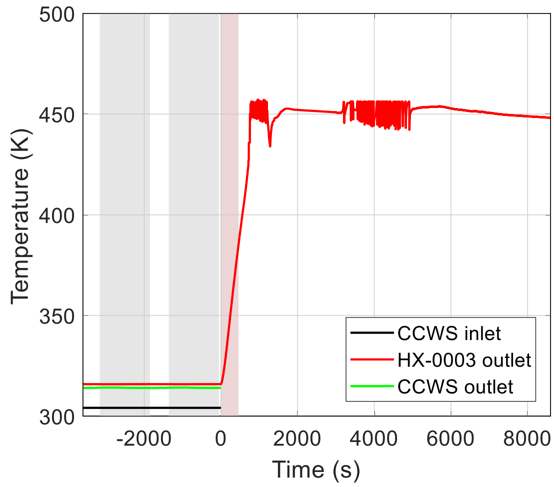

Figure 9. CCWS: relevant temperatures

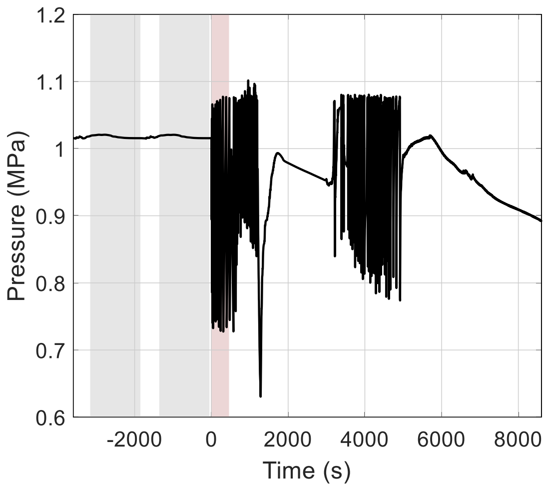

Figure 10. CCWS: pressure

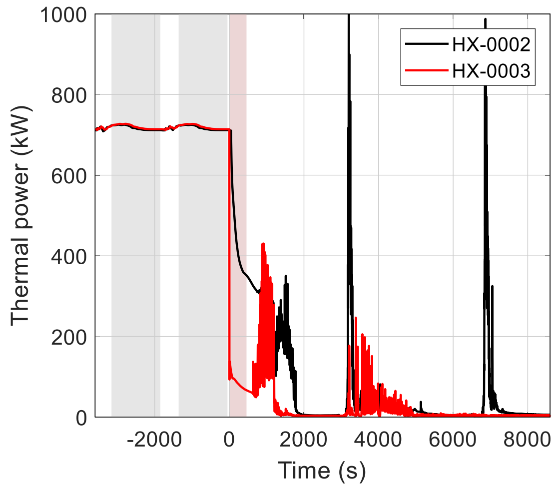

Figure 11. WCS SL: power balance

Figure 12 shows three relevant temperatures within the WCS secondary loop. The green line represents water temperature at the HX-0003 outlet plenum. The HX-0003 power decrease leads to an increase of the water temperature. At this time, SL pump is still in operation. The small step observed in the secondary flow rate after the PIE (see Figure 13) is due to the water density change. The mass flow rate is kept at around 4.15 kg/s over the full power flat-top condition and the temperature increase is also detected within the HX-0002. At 1200 s HX-0003 outlet temperature reaches the maximum temperature of 475 K, which corresponds to SL pump cut off setpoint. Thus, the component is stopped and the mass flow rate decreases to zero in 15 s (Figure 13). A quick temperature decrease is observed in both the sides of the HX-0003. As a consequence of the secondary pump trip, the power removed by the HX-0003 decreases, leading to the reduction of the boiling rate within the isolated section of the CCWS. The pressure decreases to the minimum value of 0.63 MPa (1282 s from the PIE, Figure 10) and remains below the safety valve opening setpoint up to 3200 s. The negative gradient of the pressure is due to the heat losses, which exceeds the HX-0003 power.

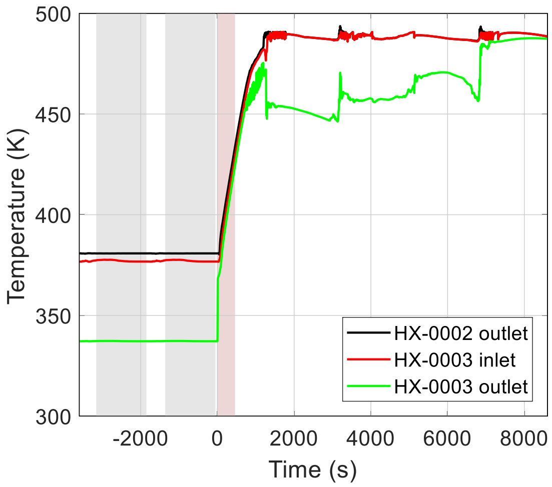

Figure 12. WCS SL: relevant temperatures

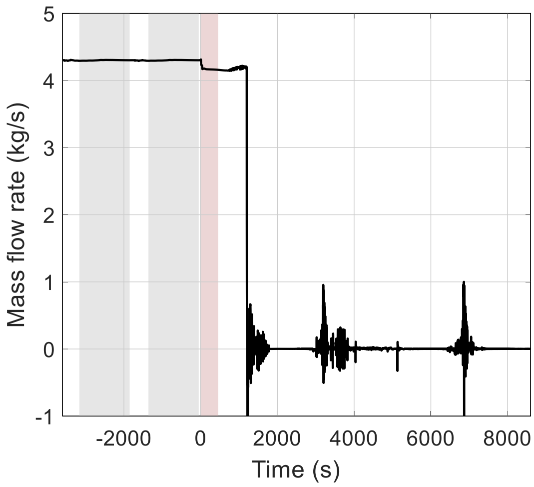

Figure 13. WCS SL: mass flow rate

On the WCS SL, as the pump cuts off, pressure increases reaching the PORV opening set point at 1220 s (Figure 14). It is followed by repeated opening and closing cycles up to 1774 S. After that, power removed from the system (HX-0003 power and heat losses) exceeds supplied power (HX-0002 power and PRZ heater), explaining the negative gradient of the SL pressure up to 3120 s. HX-0002 continues to exchange power, increasing steam fraction within the shell side. At 2950 s almost the total amount of water within the HX-0002 shell reaches the vapor phase, causing a quick increase of the SL pressure. SL PORV opens at 3175 s, causing the mass flow peaks observed in Figure 13. The HX-0003 power increases (see red line in Figure 11), leading to repeated opening and closing cycles of the CCWS safety valve (see pressure fluctuations between 3210 and 4920 s, Figure 10). After that, HX-0003 power remains below the CCWS heat losses up to the end of the simulation. On the WCS SL, the PORV opening leads to a high peak of the HX-0002 power, that is repeated at 6865 s.

Regarding the WCS primary loop, after the PIE, HX-0002 power decrease leads to the temperature increase at the HX-0002 outlet (Figure 15). The effect of the SL PORV openings is visible in the two consecutive temperature low peaks observed at the outlet plena of the HX-0001 and the HX-0002. The temperature control system regulates the power supplied by the HT-0001 (green line in Figure 16), ensuring the almost constant temperature of 568 K at the TBM inlet (Figure 17). In comparison with the previous scenario, temperature peaks at the TBM inlet and outlet sections are lower. The maximum temperature reached after the PIE does not exceed the nominal maximum value. In addition, concerning the PbLi loop, temperature control system guarantees a satisfactory margin from the freezing point.

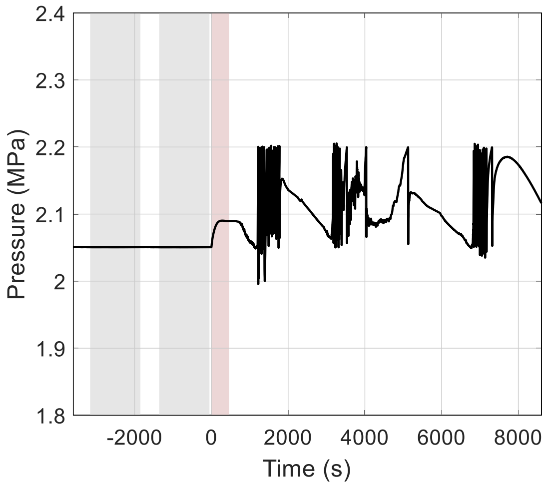

Figure 14. WCS SL: pressure

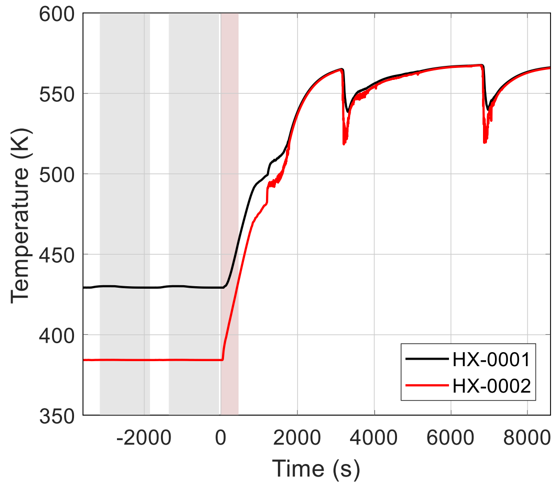

Figure 15. WCS PL: HXs tube side outlet temperatures

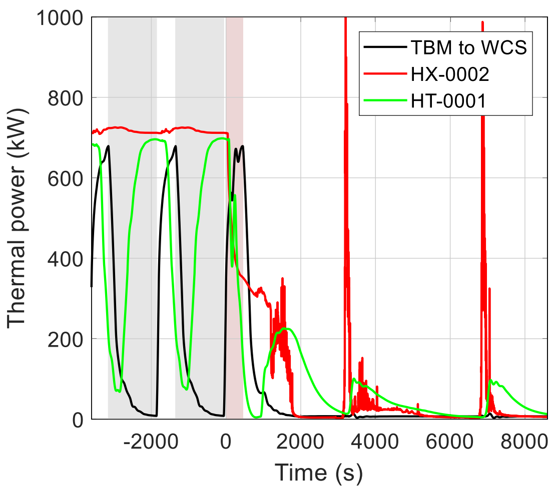

Figure 16. WCS PL: power balance

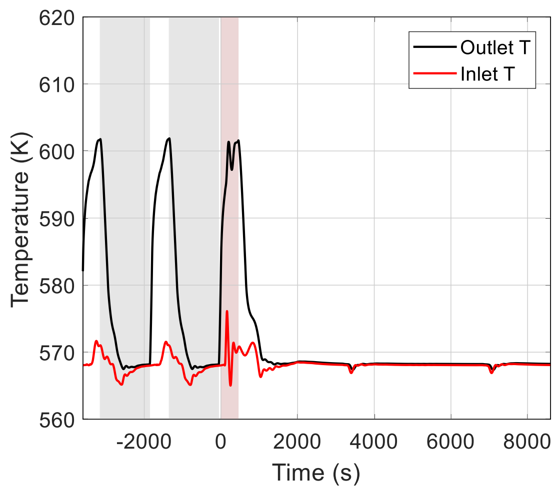

Figure 17. WCS PL: TBM inlet and outlet temperatures

4 Conclusions

The present paper deal with the presentation of the WCLL-TBS WCS conceptual design. Furthermore, a computational activity has been promoted to assess system thermal-hydraulic capabilities, and the main simulation outcomes has been summarized.

The conceptual design has been developed at DIAEE of “Sapienza” University of Rome, in collaboration with ENEA. Considering the DEMO BB relevancy of the ITER WCLL TBM, the same thermodynamic conditions have been considered for the primary coolant. The WCLL-TBS WCS consists of a primary and a secondary loop. The PL deals with the direct heat removal from the TBM and the SL introduces a physical barrier between WCS PL and CCWS, to avoid its contamination. With the aim to prevent excessive temperature difference between the WCS cold branch and the CCWS, an economizer is foreseen at the PL center, resulting in a “eight” shape loop. Pressure and temperature control systems are foreseen. The first one is basically composed of two steam bubble pressurizers (one per each loop), equipped with heater bank, spray system, PORV and SRV while the temperature control system ensures the required water conditions at TBM inlet section, in both BOL and EOL pulsed regimes. It is realized with HX bypass systems and with the electric heater installed upstream the TBM inlet.

The computational activity has been performed with a modified version of the RELAP5 Mod3.3 system code, containing some improvements relevant for the application in fusion problems. Particular attention has been given to the WCS nodalization scheme. It includes primary and secondary loops and the CCWS section placed within the TCWS Vault. In addition, a detailed model of the PbLi loop and of the TBM have been developed, to verify the requirements under normal and abnormal operations.

Firstly, a steady state calculation has been performed, reproducing the full power flat-top condition. The agreement observed between nominal data and computational results demonstrates the model capability of reproducing the whole system TH behavior. The main differences between BOL and EOL operations have been highlighted, mainly regarding the operation of the temperature control system (i.e., the mass flow through the heat exchangers bypass). The main requirements at the TBM inlet, in terms of mass flow and temperature, are respected for both water coolant (3.74 kg/s at 568.15 K) and liquid breeder (0.65 kg/s at 568.15 K). Once characterized the full power flat top, NOS operational state has been investigated. Simulations outcomes have demonstrated the capabilities of the pressure and temperature control systems to match the required water and PbLi conditions at TBM inlet. For water coolant, fluctuations are limited to +/- 3 K, acceptable for WCS and TBM operation. Moreover, it has been verified that in any part of the PbLi loop an adequate margin (16 K) from the freezing point is maintained. Finally, a preliminary transient analysis has been performed, selecting a LOHS (loss of flow in the CCWS) as abnormal scenario for that study. In this abnormal condition TBM cooling is ensured. Water and PbLi conditions at the TBM inlet sections are kept close to the required values. A negligible temperature increase (few degrees) occurs on the FW structure, avoiding any damage.

Acknowledgments

The authors wish to thank Gianfranco Caruso for his guide, assistance and support during the development of this research work and for the valuable review of the present paper. A special thanks to Alessandro Del Nevo and Italo Ricapito for the technical contribute and the supervision during the progress of the design and simulation activities. This work has been carried out within the framework of the EUROfusion Consortium and has received funding from the Euratom research and training programme 2014-2018 and 2019-2020 under grant agreement No 633053. The views and opinions expressed herein do not necessarily reflect those of the European Commission.

List of Acronyms

BB	Breeding Blanket
BOL	Beginning Of Life
BP	Back Plate
BZ	Breeder Zone
BU	Breeding Unit
CCWS	Component Cooling Water System
CPS	Coolant Purification System
CT	Cold Trap
CV	Control Volume
CVCS	Chemical Volume Control System
DEMO	DEMOnstration fusion power plant
DIAEE	Department of Astronautical, Electrical and Energy Engineering
DWT	Double Wall Tube
ENEA	Italian National Agency for New Technologies, Energy and Sustainable Economic Development
EOL	End Of Life
EU	European
FPSS	Fast Plasma Shutdown System
FW	First Wall
HR	Heating Rod
HTC	Heat Transfer Coefficient
HX	Heat eXchanger
ID	Inner Diameter
ITER	International Thermonuclear Experimental Reactor
LOHS	Loss Of Heat Sink
MHD	Magnetohydrodynamic
NAS	Neutron Activation System
NOS	Normal Operation State
OD	Outer Diameter
PbLi	Lead-Lithium
PC	Port Cell
PHTS	Primary Heat Transfer System
PI	Proportional/Integral
PIE	Postulated Initiating Event

PL	Primary Loop
PORV	Pilot Operated Relief Valve
PRZ	Pressurizer
PRT	Pressure Relief Tank
PWR	Pressurized light-Water moderated and cooled Reactor
QST	Quantum and radiological Science and Technology
RELAP	Reactor Excursion and Leak Analysis Program
SL	Secondary Loop
SRV	Safety Relief Valve
TAS	Tritium Accountancy System
TBM	Test Blanket Module
TBS	Test Blanket System
TES	Tritium Extraction System
TEU	Tritium Extraction Unit
TH	Thermal-Hydraulic
VS	Vertical Shaft
WCCB	Water Cooled Ceramic Breeder
WCLL	Water Cooled Lead Lithium
WCS	Water Cooling System

References

[1] A. Del Nevo et al., Recent progress in developing a feasible and integrated conceptual design of the WCLL BB in EUROfusion project, Fusion Eng. Des. 146 (2019) 1805-1809. https://doi.org/10.1016/j.fusengdes.2019.03.040.

[2] F. A. Hernández et al., 2020. Consolidated design of the HCPB Breeding Blanket for the pre-Conceptual Design Phase of the EU DEMO and harmonization with the ITER HCPB TBM program. Fusion Eng. Des. 157, 111614. https://doi.org/10.1016/j.fusengdes.2020.111614.

[3] G. Federici et al., An overview of the EU breeding blanket design strategy as an integral part of the DEMO design effort, Fusion Eng. Des. 141 (2019) 30-42. https://doi.org/10.1016/j.fusengdes.2019.01.141.

[4] L. M. Giancarli et al., 2020. Overview of recent ITER TBM Program activities. Fusion Eng. Des. 158, 111674. https://doi.org/10.1016/j.fusengdes.2020.111674.

[5] I. Ricapito et al., 2020. European TBM programme: First elements of RoX and technical performance assessment for DEMO breeding blankets. Fusion Eng. Des. 156, 111584. https://doi.org/10.1016/j.fusengdes.2020.111584.

[6] A. Aiello et al., Updated design and integration of the ancillary circuits for the European Test Blanket Systems, Fusion Eng. Des. 146 (2019) 27-30. https://doi.org/10.1016/j.fusengdes.2018.11.015.

[7] A. Tincani et al., Conceptual design of the main Ancillary Systems of the ITER Water Cooled Lithium Lead Test Blanket System. Fusion Eng. Des. 167, 2021, 112345. https://doi.org/10.1016/j.fusengdes.2021.112345.

[8] I. Ricapito et al., Tritium technologies and transport modelling: main outcomes from the European TBM Project, Fusion Eng. Des. 136 (2018) 128-134. https://doi.org/10.1016/j.fusengdes.2018.01.023.

[9] M. Utili et al., Tritium Extraction from HCLL/WCLL/DCLL PbLi BBs of DEMO and HCLL TBS of ITER, IEEE Transactions on Plasma Science, 47 (2019), 1464-1471. https://doi.org/10.1109/TPS.2018.2886409.

[10] Y. Kawamura et al., Status of water cooled ceramic breeder blanket development, Fusion Eng. Des. 136 (2018) 1550-1556. https://doi.org/10.1016/j.fusengdes.2018.05.055.

[11] L. M. Giancarli et al., Overview of the ITER TBM Program, Fusion Eng. Des. 87 (2012) 395-402. https://doi.org/10.1016/j.fusengdes.2011.11.005.

[12] E. Martelli et al., Thermal-hydraulic modeling and analyses of the water-cooled EU DEMO using RELAP5 system code, Fusion Eng. Des 146 (2019) 1121-1125. https://doi.org/10.1016/j.fusengdes.2019.02.021.

[13] A. Tarallo et al., PMI-7.1.2. Phase II - Task 2 Design-T004-D001 (D2.4) Detail Model of the WCLL-TBS ancillary systems. H2020 EUROfusion Technical Report, IDM Ref. 2PA9XE

[14] The American Society of Mechanical Engineers (ASME), Boiler and Pressure Vessel Code, Section II, Part D, Properties (Metric), 2015 Edition, New York (NY).

[15] Promat International N.V., Technical datasheet for MICROTHERM® MPS Insulator Material, 2017, https://www.promat.com/en/industry/

[16] The American Society of Mechanical Engineers (ASME), Boiler and Pressure Vessel Code, Section III, Division 1, Subsection NC, 3324.3, New York, 2015.

[17] M. A. Kreider et al., A global fouling factor methodology for analyzing steam generator thermal performance degradation, International Steam Generator and Heat Exchanger Conference, Toronto, Canada, 1998. Available online: https://inis.iaea.org/search/search.aspx?orig_q=RN:30031799.

[18] T. Prusek et al., A methodology to simulate the impact of tube fouling on steam generator performance with a thermal-hydraulic code, Proceedings of International Conference on Heat Exchanger Fouling and Cleaning, Enfield (Dublin), Ireland, 07-12 June 2015. Available online: http://www.heatexchanger-fouling.com/papers/papers2015/17_Prusek_F.pdf.

[19] The American Society of Mechanical Engineers (ASME), Welded and Seamless Wrought Steel Pipe, Section B36.10M, New York, 1995.

[20] N. E. Todreas and M. S. Kazimi, Nuclear Systems Volume I. Thermal Hydraulic Fundamentals, second ed., Taylor & Francis Inc, 2011, ISBN:1439808872.

[21] Watlow® Electric Manufacturing Company, Datasheet for Pressurizer heaters. https://www.watlow.com/resources-and-support/technical-library/specification-sheets, 2015.

[22] D. Q. Kern, Process Heat Transfer, 21st ed., McGraw-Hill International Book Company, 1983, ISBN 0-07-085353-3.

[23] USNRC. RELAP5/MOD3 Code Manual Volume I: Code Structure, System Models, and Solution Methods, NUREG/CR-5535, Washington DC., 1998.

[24] F. Giannetti et al., Development of a RELAP5 mod3.3 version for FUSION applications. DIAEE Sapienza Technical Report D1902_ENBR_T01 Rev. 01.

[25] D. Martelli et al., Literature review of lead-lithium thermophysical properties, Fusion Eng. Des. 138 (2019) 183-195. https://doi.org/10.1016/j.fusengdes.2018.11.028.

[26] R. A. Seban and T. T. Shimazaki, Heat transfer to a fluid flowing, Trans. Am. Soc. Mech. Eng. 73 (1951) 803-809.

[27] C. Ciurluini et al., 2020. Thermal-hydraulic modeling and analysis of the Water Cooling System for the ITER Test Blanket Module. Fusion Eng. Des. 158, 111709. https://doi.org/10.1016/j.fusengdes.2020.111709.

[28] I. E. Idelchik, Handbook of Hydraulic Resistance, 4th ed., Begell House, Inc., 2007, ISBN 978-1567002515.

[29] Julien Aubert et al., 2020, Design and Preliminary Analyses of the New Water Cooled Lithium Lead TBM for ITER. Fusion Eng. Des. 160, 111921. https://doi.org/10.1016/j.fusengdes.2020.111921.

[30] L. Melchiorri et al., Development of a RELAP5/MOD3.3 module for MHD pressure drop analysis in liquid metals loops, submitted to Nucl. Fusion.